Compartmental Glycosylation Flux Analysis

Shilpi Aggarwal*. Xin Qi. Sriram Neelamegham***.
Rudiyanto Gunawan******

**Department of Chemical and Biological Engineering, University at Buffalo,
Buffalo, NY 14260 USA (e-mail: shilpiag@buffalo.edu).
** Department of Chemical and Biological Engineering, University at Buffalo,
Buffalo, NY 14260 USA (e-mail: qixin@buffalo.edu).
*** Department of Chemical and Biological Engineering, University at Buffalo,
Buffalo, NY 14260 USA (e-mail: neel@buffalo.edu).
****Department of Chemical and Biological Engineering, University at Buffalo,
Buffalo, NY 14260 USA (e-mail: rgunawan@buffalo.edu).*

Abstract: N-linked glycosylation is a critical quality attribute of therapeutic monoclonal antibodies (mAbs) – an important class of biologics. In this work, we developed compartmental Glycosylation Flux Analysis (cGFA) to enable a more accurate representation of the cell's Golgi apparatus (GA), where protein glycosylation takes place, in the analysis of intracellular fluxes of glycosylation reactions. The application of one-compartment and two-compartment cGFA to a Chinese hamster ovary cell culture production of immunoglobulin G demonstrated the insufficiency of modeling the GA as one well-mixed compartment. The two-compartment cGFA was able to, not only fit the data significantly better than the one-compartment cGFA, but also accurately predict the localization of enzyme in the GA cisternae. Information on glycosylation alterations during cell cultivation, as provided by the cGFA, may lead to a better understanding of how different cell culture parameters control the N-linked glycosylation which would enable a more precise glycoengineering of therapeutic mAbs.

Keywords: glycosylation, flux analysis, monoclonal antibodies, Chinese hamster ovary.

1. INTRODUCTION

There has been a rapid increase in the demand and production of therapeutic glycoproteins, especially monoclonal antibodies (mAbs) (Niwa and Satoh, 2015). Global sales of mAbs reached $115 billion in 2018, and is projected to exceed $300 billion by 2025 (Lu *et al.*, 2020). Therapeutic mAbs are predominantly produced by using mammalian cell cultures to ensure human-compatible products. One critical quality attribute of mAb drugs is their N-linked glycosylation – a post-transcriptional modification involving the attachment of nucleotide sugar molecules to the arginine residue in the fragment crystallizable region (Krambeck and Betenbaugh, 2005). N-linked glycosylation of mAbs affects their stability, folding (Aebi, 2013), clearance (Solá and Griebenow, 2010), bioactivity (Jefferis, 2009), and immunogenicity (Harding *et al.*, 2010, Hutter *et al.*, 2017). Since protein glycosylation is a non-template driven process, involving a network of enzymatic reactions in the cell's Golgi apparatus (GA), there exists a heterogeneity in the glycan structure attached to a glycoprotein produced by cells. A family of glycoproteins that differs only in the glycan structures are here referred to as glycoforms, while the distribution of glycoforms is referred to as the glycosylation profile or glycan profile.

The US Food and Drug Administration (FDA) requires a report on the glycan profile as a part of the drug approval process of glycoprotein-based biologics (FDA, 2004). The control of N-linked glycan profile is thus imperative in the biomanufacturing of therapeutic glycoproteins. For this reason, mathematical modeling of N-linked glycosylation has been actively pursued to understand how different cell culture parameters, including culture media composition, supplements, pH, temperature, dissolved oxygen, and cell host, affect the glycan profile (Umaña and Bailey, 1997, Krambeck *et al.*, 2009, Jimenez del Val *et al.*, 2011, Jiménez del Val *et al.*, 2013, Jedrzejewski *et al.*, 2014, Spahn *et al.*, 2016, Spahn *et al.*, 2017, Hutter *et al.*, 2017, Hutter *et al.*, 2018). Notably, parameter-free stoichiometric constraint-based models (CBMs) have recently been used to evaluate intracellular glycosylation fluxes (reaction rates) from cell culture concentration data of glycan profiles (Hutter *et al.*, 2017, Hutter *et al.*, 2018, Spahn *et al.*, 2016). Parameter-free models avoid many issues in more complex differential equation-based models that require estimating a large number of unknown kinetic parameters. However, the assumption that protein glycosylation in GA occurs in a well-mixed volume in these parameter-free models is inconsistent with how glycosylation enzymes are non-uniformly distributed across the GA cisternae (Villiger *et al.*, 2016).

In this work, we modified and expanded the capability of our recently proposed method, called Glycosylation Flux Analysis (GFA) (Hutter et al., 2017, Hutter et al., 2018), to better capture how the compartmentalization of GA affects glycosylation. As illustrated in Figure 1a, we developed a compartmental flux balance model of the N-linked glycosylation process that enables the prediction of
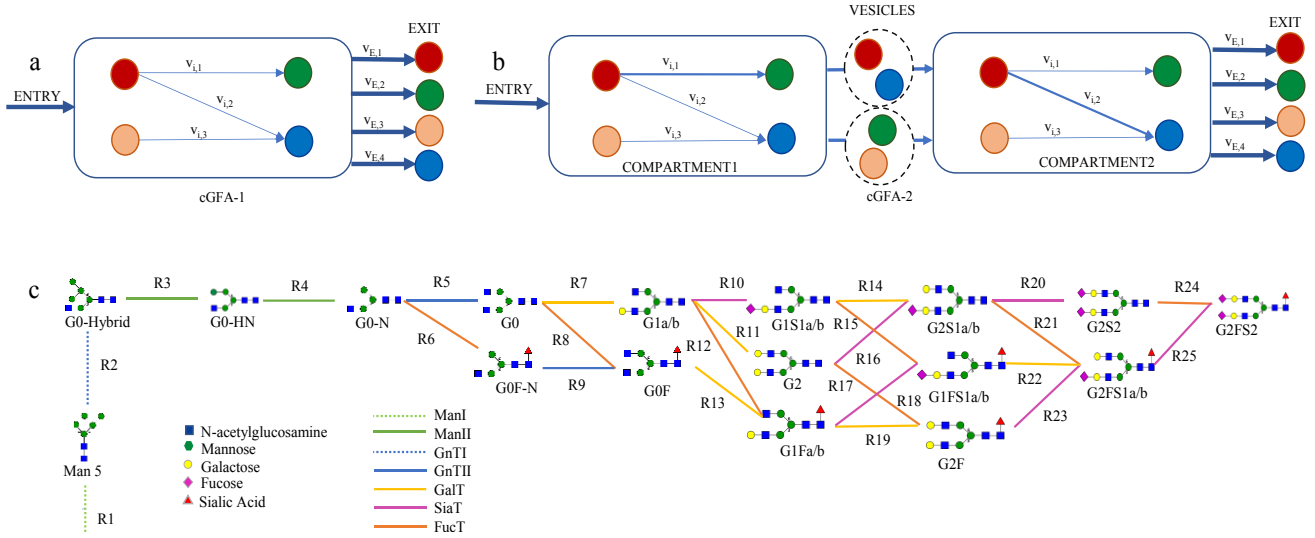
Fig. 1. (a) Single and (b) multi-compartmental Glycosylation Flux Analysis. (c) N-linked glycosylation network of IgG (Neelamegham *et al.*, 2019). Reactions with the same colored arrows are catalyzed by the same enzyme.

glycosylation fluxes in GA compartments. We applied the compartmental GFA (cGFA) to study N-linked glycosylation of immunoglobulin-G (IgG) in fed-batch culture of Chinese Hamster Ovary (CHO) cells. We demonstrated that cGFA gives improved predictions for the cell-specific secretion rates of IgG glycoforms over non-compartmental GFA. Further, cGFA is able to accurately predict the distribution of glycosylation enzymes in the two GA compartments.

2. MATERIALS AND METHODS

2.1 Experimental Data

Time-series experimental data of IgG titer and glycan profiles were taken from a study of fed-batch CHO-K1 cell cultivation in a modified CD-CHO commercial media (Sumit *et al.*, 2019). The culture temperature and glucose level were maintained at 36.5ºC and above 1.5 g/L, respectively. The pH in the bioreactor was kept at 7.05+0.05 until Day 6, after which it was kept at 7.05+0.15. The dissolved oxygen was controlled at 40% of air saturation by micro-bubble sparing of a mixture of CO_2/air and O_2. In the cGFA, we used data of cell culture samples taken on days 3, 5, 7, 9, and 12.

2.2 Data Preprocessing

Data of IgG cell-specific productivity and IgG glycan are processed to evaluate the cell-specific secretion rates of various IgG glycoforms, which are the input for cGFA. For the fed-batch CHO case study, we used time-series data on viable cell density, $X_v(t)$, IgG titer T(t), and glycan fractions $f_i(t)$ from a previous publication (CC-2 batch in (Sumit *et al.*, 2019)). We calculated the concentrations of different IgG glycoforms at each time point as follows:

$$c_{E,i}(t_k) = f_i(t_k)T(t_k) \tag{1}$$

where $c_{E,i}(t_k)$ is the extracellular concentration of the ith glycoform at the kth time point t_k. In order to reduce the impact of noise in computing the glycoform secretion fluxes, we smoothened the glycoform concentrations using a Hill-type function:

$$\hat{c}_{E,i}(t) = \frac{a}{\frac{b^n}{t} + d} \tag{2}$$

where the parameters *a*, *b*, *d*, and *n* were estimated using the `fit` function in MATLAB. We smoothened the viable cell density data using the logistic function:

$$\hat{X}_v(t) = \frac{A}{e^{Bt} + Ce^{-Dt}} \tag{3}$$

where the parameters *A*, *B*, *C*, and *D* were again estimated using the `fit` function in MATLAB. We used the smoothened functions above to compute the secretion rates of individual IgG glycoforms, as follows:

$$v_{E,i}^M(t_k) = \frac{1}{\hat{X}_v(t_k)} \frac{d\hat{c}_{E,i}(t)}{dt}\Bigg|_{t=t_k} \tag{4}$$

2.3 N-linked Glycosylation

N-linked glycosylation involves a network of enzymatic reactions and a heterogeneous set of glycoforms (Krambeck and Betenbaugh, 2005). The heterogeneity of glycoforms arises because enzymatic glycosylation reactions in the GA follow a non-template-driven process that is not controlled at the DNA level. The GA comprises several stacked pouches or cisternae that form different compartments – cis, medial, and trans-GA. Glycosylation enzymes are distributed non-uniformly across the GA cisternae (Kornfeld and Kornfeld, 1985), motivating the present work. Specifically, we evaluated two scenarios of cGFA, in which the GA is modeled as a single compartment and as two compartments.

2.4 Compartmental Glycosylation Flux Analysis

The cGFA uses a stoichiometric CBM to evaluate the intracellular flux distribution in the glycosylation network using the cell-specific secretion rates of glycoforms. The original GFA method (Hutter *et al.*, 2017) is based on the flux balance equation for various glycoform species in the glycosylation network, which requires only the stoichiometry of the glycosylation reactions, as follows:

$$\frac{dc_{I,i}}{dt} = \sum_{j=1}^{n} S(i,j)v_{I,j} - v_{E,i} \tag{5}$$

where, $c_{I,i}$ denotes the intracellular concentration of the ith glycoform, $S(i,j)$ denotes the stoichiometric coefficients of the ith glycoform in the jth glycosylation reaction, $v_{I,j}$ denotes the intracellular flux (rate) of the jth reaction, and $v_{E,i}$ denotes the cell-specific secretion rate for the ith glycoform. The stochiometric coefficient of $S(i,j)$ has a negative (positive) sign if the reaction consumes (produces) the ith glycoform. By using the pseudo-steady state assumption (setting $\frac{dc_{I,i}}{dt}$ to zero), the flux balance in (5) for the glycoforms reduces to a system of linear equations describing the relationship between the intracellular glycosylation fluxes $v_I(t_k)$ and the cell-specific secretion fluxes $v_E(t_k)$ at any measurement time point t_k as follows:

$$Sv_I(t_k) - v_E(t_k) = 0 \tag{6}$$

where, S is an $m \times n$ matrix of stoichiometric coefficients for the glycosylation network with m glycoforms and n intracellular glycosylation reactions. The pseudo-steady state assumption above is analogous to the implementation of dynamic flux balance analysis (Mahadevan *et al.*, 2002). The assumption is justified by the fact that the residence time of the glycoforms in the Golgi apparatuses (~20 -40 minutes (Bibila and Flickinger, 1991, Hirschberg and Lippincott-Schwartz, 1999)) is much shorter than the time-scale of the dynamic changes in the cell culture. The (i,j)-th element of S is the stoichiometric coefficient of the ith glycoform in the jth reaction.

The intracellular glycosylation fluxes depend on a number of factors such as the enzyme activity, substrate concentration, and enzyme's affinity for the substrate. Following the Michaelis Menten's (MM) kinetics, the rate of an enzymatic reaction can be expressed as

$$v_{I,j}(t) = \frac{V_{max,j}(t)c_{I,i(j)}(t)}{K_m + c_{I,i(j)}(t)} \tag{7}$$

where V_{max} is the maximum rate (flux) achievable at a saturating concentration of the substrate, K_m denotes the Michaelis constant, and $c_{I,i(j)}$ denotes the concentration of the substrate glycoform for the reaction j. The maximum rate V_{max} is proportional to the enzyme concentration and the turnover number k_{cat} of the enzyme. At $c_{I,i} \ll K_m$, the MM kinetics reduces to:

$$v_{I,j}(t) = \frac{V_{max,j}(t)c_{I,i(j)}(t)}{K_m} \tag{8}$$

In the cGFA, dynamical changes of intracellular glycosylation fluxes during the cell cultivation are described by the ratio between the flux at time point t_k and that at an arbitrarily chosen reference time point t_{ref} (usually the first time point), as follows:

$$v_{I,j}(t_k) = \frac{V_{max,j}(t_k)}{V_{max,j}(t_{ref})} \frac{c_{I,i(j)}(t_k)}{c_{I,i(j)}(t_{ref})} v_{I,j}(t_{ref}) \tag{9}$$

$$v_{I,j}(t_k) = \alpha_j(t_k)\beta_{i(j)}(t_k) v_{i,j}^{ref} \tag{10}$$

where $\alpha_j(t_k)$ captures enzyme-specific changes and $\beta_{i(j)}(t_k)$ captures glycan substrate-specific alterations. The enzyme-specific factor $\alpha_j(t_k)$ is the same among reactions sharing the same enzyme, while the glycan substrate-specific factor $\beta_{i(j)}(t_k)$ is shared among all reactions sharing the same glycoform substrate. Note that the cGFA formulation above differs from the original GFA, where $\beta_i(t_k)$ is set to the same value for all glycoforms that is equal to the ratio of the cell specific productivity between the time point t_k and t_{ref}. In cGFA, the factor $\beta_i(t_k)$ in the trans-GA compartment can be evaluated from the ratio of secretion fluxes of the corresponding glycoform, by assuming that the secretion rate of a glycoform is linearly dependent on the intracellular concentration $c_{I,i}$:

$$v_{E,i}(t) = k_{T,i}c_{I,i}(t) \tag{11}$$

where $k_{T,i}$ denotes the secretion rate constant. Thus, given data of the cell-specific glycoform secretion flux $v_{E,i}^M$, $\beta_i(t_k)$ can be computed using the formula:

$$\beta_i(t_k) = \frac{c_{I,i}(t_k)}{c_{I,i}(t_{ref})} = \frac{k_{T,i}c_{I,i}(t_k)}{k_{T,i}c_{I,i}(t_{ref})} = \frac{v_{E,i}^M(t_k)}{v_{E,i}^M(t_{ref})} \tag{12}$$

The details on the cGFA using one and two compartmental modeling are given below.

2.4.1. Single compartment cGFA

In this scenario (cGFA-1), the GA is modeled as a single well-mixed reactor volume, as illustrated in Figure 1a. Given the values for $v_{E,i}(t_k)$, we evaluated $\beta_i(t_k)$ using (12). The unknown factors $\alpha_j(t_k)$ and the reference glycosylation flux $v_{i,j}^{ref}$ are estimated by the following least square regression:

$$\min_{\alpha_j(t_k), v_{i,j}^{ref}} \Phi = \sum_{i=1}^{m} \left(v_{E,i}^M - v_{E,i}\right)^2 \tag{13}$$

where $v_{E,i}$ is the cell-specific secretion flux of the ith glycoform computed using the pseudo-steady state molar balance in (6) with the intracellular glycosylation reactions set by (10). The regression problem in (13) contains $n + n_J(k-1)$ unknowns, where n is the number of intracellular glycosylation reaction, n_J is the number of enzymes involved in the glycosylation network, and k is the total number of experimental time points.
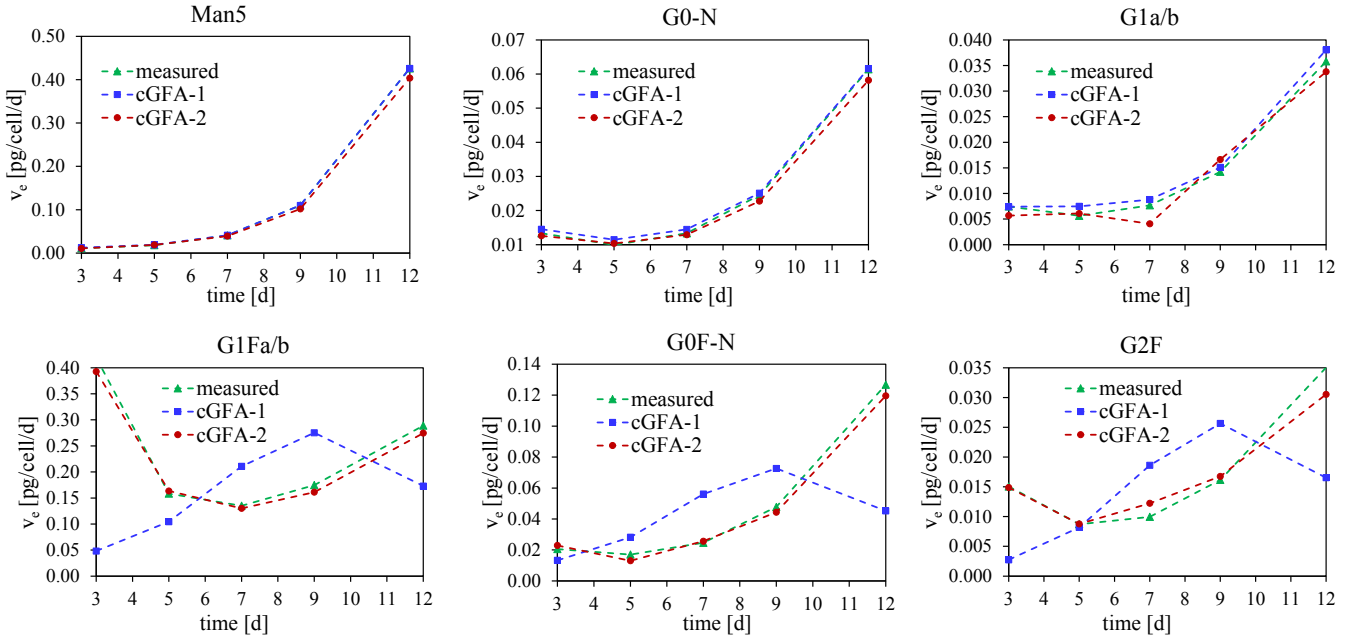
Fig. 2. Secretion fluxes of select IgG glycoforms from experimental measurements and from cGFA-1 and cGFA-2.

2.4.2. Two compartment cGFA

In this scenario (cGFA-2), the GA is modeled as two well-mixed reactor volumes connected in series. As illustrated in Figure 1b, glycoforms from the first compartment (A) are transferred entirely to the second compartment (B), while extracellular secretion of glycoforms occurs only from the second (last) compartment. Thus, we have the following modified flux balance equations (for each glycoform i):

$$0 = \sum_{j=1}^{n} S(i,j)v_{I,j}^{A} - v_{Tr,i}^{AB} \qquad (14)$$

$$0 = \sum_{j=1}^{n} S(i,j)v_{I,j}^{B} + v_{Tr,i}^{AB} - v_{E,i} \qquad (15)$$

where the superscripts A and B denote the compartments. The flux $v_{Tr,i}^{AB}$ refers to the transport from compartment A to B, which is assumed to be linearly dependent on the glycoform concentration in A. The enzyme specific factor $\alpha_j(t_k)$ is set the same for all reactions with the same enzyme, regardless of the compartment. Enzyme localization to compartments is captured by estimating two sets of $v_{i,j}^{ref}$. The factors $\beta_i^{B}(t_k)$ in the second compartment are computed from the secretion fluxes as described in (12). The unknown values $\beta_i^{A}(t_k)$, $\alpha_j(t_k)$, $v_{i,j}^{ref,A}$, and $v_{i,j}^{ref,B}$ are estimated using the least square regression:

$$\min_{\beta_i^{A}(t_k),\alpha_j(t_k),v_{i,j}^{ref,A},v_{i,j}^{ref,B}} \Phi = \sum_{i=1}^{m}\left(v_{E,i}^{M} - v_{E,i}^{B}\right)^2 \qquad (16)$$

In total, there are $2n + n_J(k - 1) + m(k - 1)$ unknowns. While no constraints were put on $v_{i,j}^{ref,A}$ and $v_{i,j}^{ref,B}$ in our implementation, one can incorporate data on the glycosylation enzyme distribution as constraints on $v_{i,j}^{ref}$ in the compartments when solving the regression problem.

3.1 N-linked Glycosylation Network

The reaction network involved in the IgG N-linked glycosylation for the case study was reconstructed to include all glycoforms that were detected in the experiment and any intermediate species that were needed to produce all detectable glycoforms (Zhou and Neelamegham, 2020). The IgG glycosylation network as depicted in Figure 1c comprises 17 glycoforms and 25 reactions. The network includes 7 enzymes: ManI, ManII, GnTI, GnTII, FucT, GalT, and SiaT. In the two-compartment cGFA, we employed the same glycosylation network in both compartments.

3.2 GFA of CHO batch cultivation

In the cGFA application, we set the cell-specific secretions rates ($v_{E,i}$) of glycoforms that were not detected in the experiment but appeared in the glycosylation network to zero, and their corresponding $\beta_i(t_k)$ to 1. Figure 2 depicts the cell-specific secretion rates of a select set of glycoforms in CHO-K1 cell cultivation (Sumit *et al.*, 2019) (see Materials and Methods). The secretion rates produced by least square regressions in cGFA-1 and cGFA-2 are also shown in Figure 2, indicating that the two-compartment cGFA-2 gives a much better agreement $\Phi = 2.2 \times 10^{-4}$ with the experimental secretion rates than the one-compartment cGFA-1 ($\Phi = 1.8 \times 10^{-1}$). While cGFA-1 is able to provide similar
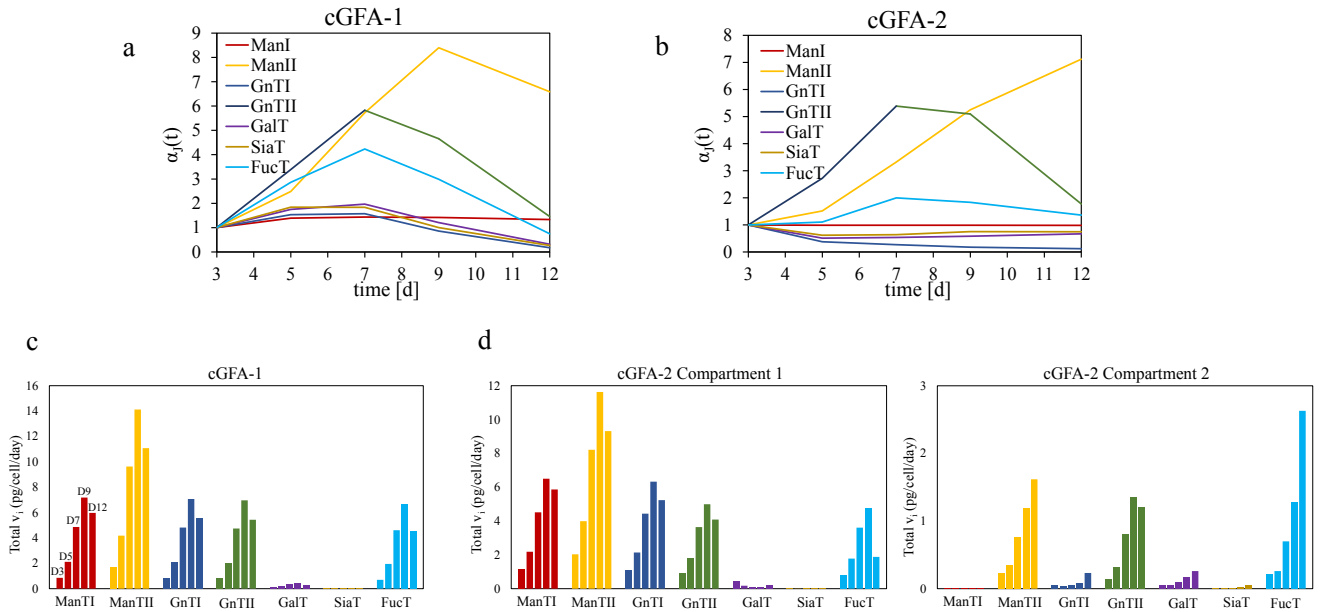
Fig. 3. cGFA of IgG production by fed-batch CHO-K1 cell culture. (a-b) Enzyme-specific factor from (a) cGFA-1 and (b) cGFA-2. (c-d) Total glycosylation fluxes for each enzyme from cGFA-1 over cultivation days from (c) cGFA-1 and

goodness of fit to cGFA-2 for some glycoforms (see top row of Figure 2), the data fitting for other glycoforms is visibly much poorer in cGFA-1 than in cGFA-2 (see bottom row of Figure 2). Importantly, for the second set of glycoforms, cGFA-1 is unable to reproduce even the general trend of secretion rate, indicating a potential issue with the modeling of the GA as a single well-mixed compartment.

Figure 3a-b shows the enzyme-specific factor $\alpha_j(t)$ for various enzymes estimated by cGFA-1 and cGFA-2. Overall, ManII displays an increase in activity over the cell cultivation along with the increase in cell-specific productivity of IgG. The two N-acetyl-glucosaminyltransferases GnTI and GnTII exhibit a transient increase in activity until day 7, followed by a decrease. The activity of glycosyltransferase enzymes that attach fucose (FucT), galactose (GalT), and sialic acid (SiaT) have a general decreasing trend over time according to both cGFA-1 and cGFA-2, with the cGFA-2 predicting a drop at earlier time points.

Figure 3c-d further illustrates the total glycosylation fluxes over time for each enzyme. Note that the total flux carried out by an enzyme can increase while the enzyme-specific factor $\alpha_j(t)$ decreases. While seemingly counterintuitive, this observation follows directly from (10), which indicates that changes in the glycosylation fluxes depend not only on enzyme activity alterations but also on glycan substrate concentration dynamics. Overall, the glycosylation fluxes increase over the duration of the cell cultivation because the cell-specific productivity of IgG increases over the same period (Sumit *et al.*, 2019).

Comparing the total glycosylation fluxes between the two GA compartments from cGFA-2, we noted that fluxes of ManI/II and GnTI are mainly localized to the first compartment, while those of GalT and FucT are predominantly taking place in the second compartment. Meanwhile, fluxes carried out by GnTII

are equally distributed between the two compartments. The compartmental localization of the different glycosylation fluxes is in good agreement with the published literature (Jimenez del Val *et al.*, 2011, Rabouille *et al.*, 1995, Hartel-Schenk *et al.*, 1991, Krambeck *et al.*, 2017). Enzymes ManI, ManII, and GnTI reside mainly in the cis- and medial-GA while the enzymes GalT and SiaT mainly reside in the trans-GA. The enzymes GnTII and FucT are concentrated in both medial- and trans-GA. Note that in cGFA-2 we did not use any information regarding the localization of the glycosyltransferases. In other words, the two compartmental cGFA is able to accurately predict the localization of different glycosylation fluxes in the GA compartments.

4. DISCUSSION

In this work, we developed the compartmental GFA for flux analysis of protein glycosylation. The cGFA is based on flux balance equation that prescribes how intracellular protein glycosylation fluxes depend stoichiometrically on and thus can be evaluated using the cell-specific secretion rates of various protein glycoforms. Like metabolic flux analysis, the cGFA is based on the parameter-free CBM that requires only the stoichiometry of the reactions involved in the glycosylation network without the need for any kinetic parameters. The cGFA accounts for the dependence of glycosylation fluxes on the activity of the corresponding glycosylation enzymes and the concentrations of the glycan substrates, by way of two time-dependent factors $\alpha_j(t)$ and $\beta_i(t)$, respectively. The cGFA represents an improvement on our previous method, the GFA, in which the influence of the glycan substrate concentration is assumed to be the same for all glycosylation reactions – an assumption that may not be true in practice. Unlike the GFA, the cGFA can be used to model GA compartments, and thus more accurately describe the

partitioning of the GA cisternae in which protein glycosylation takes place.

The application of cGFA to the N-linked glycosylation of IgG in a fed-batch cell cultivation of CHO-K1 (Sumit *et al.*, 2019) demonstrated the importance of accounting for the multi-compartmental modeling of the GA in cGFA. In the cell, glycoforms migrate from one Golgi cisternae to the next, from cis-Golgi to medial to trans-Golgi, and the multi-compartmental modeling is able to better simulate the processing of N-glycosylation across the Golgi. Also, the glycosylation enzymes are not equally distributed across the Gogli compartments. In our work, the two-compartment analysis (cGFA-2) was able to give a much better agreement with the data than the one-compartment analysis (cGFA-1). Besides, cGFA-1 has difficulty in reproducing the dynamic profile of certain glycoforms (see Figure 2). Beyond the superior data fitting, as noted in the results, the two-compartmental cGFA was able to accurately recapitulate the enzyme distribution between the first (cis-medial) and second (medial-trans) compartments of the GA that has been reported in the literature (Kornfeld and Kornfeld, 1985, Krambeck and Betenbaugh, 2005, Krambeck *et al.*, 2017). There is a drawback in using a multi-compartmental model in the cGFA. First, the addition of a compartment comes at a cost of an increased number of unknown variables to be estimated, specifically n additional reference fluxes and $m(k-1)$ additional $\beta_i(t)$ values. So, a particular attention must be paid so that the least square regression problem of estimating glycosylation fluxes does not become underdetermined. As usual, there is a diminishing benefit where further addition of compartments will not improve the data fitting. In addition, the higher number of unknowns means that the least square regression in the flux analysis has a higher complexity and thus will incur a higher computational cost to solve.

5. ACKNOWLEDGEMENT

REFERENCES

Aebi, M. (2013). N-linked protein glycosylation in the ER. *Biochim Biophys Acta,* 1833**,** 2430-7.

Bibila, T. A. & Flickinger, M. C. (1991). A model of interorganelle monoclonal antibody transport and secretion in mouse hybridoma cells. *Biotechnology and Bioengineering,* 38**,** 767-780.

FDA (2004). *Guidance for industry PAT, a framework for innovative pharmaceutical development, manufacturing, and quality assurance,* Rockville, MD, U.S. Dept. of Health and Human Services, Food and Drug Administration, Center for Drug Evaluation and Research.

Harding, F. A., Stickler, M. M., Razo, J. & Dubridge, R. B. (2010). The immunogenicity of humanized and fully human antibodies: residual immunogenicity resides in the CDR regions. *MAbs,* 2**,** 256-65.

Hartel-Schenk, S., Minnifield, N., Reutter, W., Hanski, C., Bauer, C. & James Morré, D. (1991). Distribution of glycosyltransferases among Golgi apparatus subfractions from liver and hepatomas of the rat. *Biochimica et Biophysica Acta (BBA) - General Subjects,* 1115**,** 108-122.

Hirschberg, K. & Lippincott-Schwartz, J. (1999). Secretory pathway kinetics and *in vivo* analysis of protein traffic from the Golgi complex to the cell surface. *The FASEB Journal,* 13**,** S251-S256.

Hutter, S., Villiger, T. K., Brühlmann, D., Stettler, M., Broly, H., Soos, M. & Gunawan, R. (2017). Glycosylation flux analysis reveals dynamic changes of intracellular glycosylation flux distribution in Chinese hamster ovary fed-batch cultures. *Metabolic Engineering,* 43**,** 9-20.

Hutter, S., Wolf, M., Papili Gao, N., Lepori, D., Schweigler, T., Morbidelli, M. & Gunawan, R. (2018). Glycosylation Flux Analysis of Immunoglobulin G in Chinese Hamster Ovary Perfusion Cell Culture. *Processes,* 6**,** 176.

Jedrzejewski, P. M., Del Val, I. J., Constantinou, A., Dell, A., Haslam, S. M., Polizzi, K. M. & Kontoravdi, C. (2014). Towards controlling the glycoform: a model framework linking extracellular metabolites to antibody glycosylation. *Int J Mol Sci,* 15**,** 4492-522.

Jefferis, R. (2009). Glycosylation as a strategy to improve antibody-based therapeutics. *Nat Rev Drug Discov,* 8**,** 226-34.

Jiménez Del Val, I., Constantinou, A., Dell, A., Haslam, S., Polizzi, K. M. & Kontoravdi, C. (2013). A quantitative and mechanistic model for monoclonal antibody glycosylation as a function of nutrient availability during cell culture. *BMC Proceedings,* 7**,** O10.

Jimenez Del Val, I., Nagy, J. M. & Kontoravdi, C. (2011). A dynamic mathematical model for monoclonal antibody N-linked glycosylation and nucleotide sugar donor transport within a maturing Golgi apparatus. *Biotechnol Prog,* 27**,** 1730-43.

Kornfeld, R. & Kornfeld, S. (1985). Assembly of asparagine-linked oligosaccharides. *Annu Rev Biochem,* 54**,** 631-64.

Krambeck, F. J., Bennun, S. V., Andersen, M. R. & Betenbaugh, M. J. (2017). Model-based analysis of N-glycosylation in Chinese hamster ovary cells. *PLOS ONE,* 12**,** e0175376.

Krambeck, F. J., Bennun, S. V., Narang, S., Choi, S., Yarema, K. J. & Betenbaugh, M. J. (2009). A mathematical model to derive N-glycan structures and cellular enzyme activities from mass spectrometric data. *Glycobiology,* 19**,** 1163-75.

Krambeck, F. J. & Betenbaugh, M. J. (2005). A mathematical model of N-linked glycosylation. *Biotechnol Bioeng,* 92**,** 711-28.

Lu, R.-M., Hwang, Y.-C., Liu, I. J., Lee, C.-C., Tsai, H.-Z., Li, H.-J. & Wu, H.-C. (2020). Development of therapeutic antibodies for the treatment of diseases. *Journal of Biomedical Science,* 27**,** 1.

Mahadevan, R., Edwards, J. S. & Doyle, F. J. (2002). Dynamic flux balance analysis of diauxic growth in Escherichia coli. *Biophysical journal,* 83**,** 1331-1340.

Neelamegham, S., Aoki-Kinoshita, K., Bolton, E., Frank, M., Lisacek, F., Lütteke, T., O'Boyle, N., Packer, N. H., Stanley, P., Toukach, P., Varki, A., Woods, R. J. & Group, T. S. D. (2019). Updates to the Symbol Nomenclature for Glycans guidelines. *Glycobiology,* 29**,** 620-624.

Niwa, R. & Satoh, M. (2015). The current status and prospects of antibody engineering for therapeutic use: focus on glycoengineering technology. *J Pharm Sci,* 104**,** 930-41.

Rabouille, C., Hui, N., Hunte, F., Kieckbusch, R., Berger, E. G., Warren, G. & nilsson, T. (1995). Mapping the distribution of Golgi enzymes involved in the construction of complex oligosaccharides. *Journal of Cell Science,* 108**,** 1617-1627.

Solá, R. J. & Griebenow, K. (2010). Glycosylation of therapeutic proteins: an effective strategy to optimize efficacy. *BioDrugs,* 24**,** 9-21.

Spahn, P. N., Hansen, A. H., Hansen, H. G., Arnsdorf, J., Kildegaard, H. F. & Lewis, N. E. (2016). A Markov chain model for N-linked protein glycosylation--towards a low-parameter tool for model-driven glycoengineering. *Metab Eng,* 33**,** 52-66.

Spahn, P. N., Hansen, A. H., Kol, S., Voldborg, B. G. & Lewis, N. E. (2017). Predictive glycoengineering of biosimilars using a Markov chain glycosylation model. *Biotechnol J,* 12.

Sumit, M., Dolatshahi, S., Chu, A.-H. A., Cote, K., Scarcelli, J. J., Marshall, J. K., Cornell, R. J., Weiss, R., Lauffenburger, D. A., Mulukutla, B. C. & Figueroa, B. (2019). Dissecting N-Glycosylation Dynamics in Chinese Hamster Ovary Cells Fed-batch Cultures using Time Course Omics Analyses. *iScience,* 12**,** 102-120.

Umaña, P. & Bailey, J. E. (1997). A mathematical model of N-linked glycoform biosynthesis. *Biotechnology and Bioengineering,* 55**,** 890-908.

Villiger, T. K., Scibona, E., Stettler, M., Broly, H., Morbidelli, M. & Soos, M. (2016). Controlling the time evolution of mAb N-linked glycosylation - Part II: Model-based predictions. *Biotechnol Prog,* 32**,** 1135-1148.

Zhou, Y. & Neelamegham, S. (2020). Available: VirtualGlycome.org/GlycoEnzDB [Accessed 11/17/2020].